

Floquet Majorana Edge Mode and Non-Abelian Anyons in a Driven Kitaev Model

Masahiro Sato,¹ Yuki Sasaki,¹ and Takashi Oka²

¹*Department of Physics and Mathematics, Aoyama-Gakuin University, Sagamihara, Kanagawa 229-8558, Japan*

²*Department of Applied Physics, University of Tokyo, Hongo 7-3-1, Bunkyo, Tokyo 113-8656, Japan*

(Dated: February 28, 2022)

We theoretically study laser driven nonequilibrium states in the Kitaev honeycomb model with a magnetoelectric cross coupling. We show that a topological spin liquid with a gapless chiral edge mode emerges when we apply an elliptically or circularly polarized laser. This is a strongly correlated quantum spin version of the Floquet topological insulator. In the topological phase, the edge mode is made from Majorana fermions and the bulk has gapped non-Abelian anyon excitations.

PACS numbers: 75.10.Kt, 75.85.+t, 42.50.Dv

Introduction – Ultrafast manipulation of quantum systems by laser is becoming a hot topic in condensed matter [1–6]. A recent progress is its marriage with the idea of topology [7–13]. A topological many-body state is characterized by a bulk quantum number, and the hallmark is the existence of an edge state at its interface between a trivial state. Quantum systems driven by time periodic external fields, such as laser, is described by “photo-dressed” Floquet states, and its properties can be different from the original equilibrium system [5, 14–27].

In a theoretical prediction [14], it was shown that if a circularly polarized laser (CPL) is applied to two-dimensional Dirac systems, a gap opens at the Dirac point, and the system becomes a topological Hall state. This gap opening was recently observed by time resolved APRES [5]. Taking the high frequency limit, it was shown [15] that the effective static model of the honeycomb lattice in CPL is equivalent to the Haldane honeycomb model for a quantum Hall effect without Landau levels [11]. Chiral edge states induced by CPL were also experimentally observed in graphene [3, 4, 28] as well as in a photonic cousin [21].

In this paper, we propose a quantum spin version of the Floquet topological insulator in systems described

by the Kitaev honeycomb lattice model [7]. The story is parallel to the electron case [14, 15] after fermionizing the spins: The laser induces an effective *imaginary* next nearest neighbor (NNN) hopping term [see Eq. (11) later]. This plays the same role as the NNN hopping in Haldane model [11] and opens a topological gap at the Dirac cone of Majorana fermions. The Kitaev model is an anisotropic spin- $\frac{1}{2}$ model with Ising interactions $S_r^x S_{r'}^x$, $S_r^y S_{r'}^y$, and $S_r^z S_{r'}^z$, assigned to the three bonds in the honeycomb lattice. Recent studies show that it may be realized as an effective low-energy model for a Mott insulator with strong spin-orbit coupling [30, 31]. In the Kitaev honeycomb lattice model, it was shown that a spin-liquid (disordered) ground state is realized and fermionic excitations described by a single Dirac cone take place. If a gap opens at the Dirac point due to some perturbation, the Kitaev model has non-Abelian anyons with an Ising type braiding rule. Anyons and their manipulation have attracted much attention in the field of quantum computation [10]. Kitaev’s original proposal for anyons was to apply a static magnetic field [7]. The Zeeman coupling generates a term that opens a gap at the third-order perturbation level. In this work, we show that it is possible to open a gap at the Dirac point using CPL, or more generally, elliptically polarized laser (EPL) when a magnetoelectric (ME) coupling is taken into account. The virtue of this proposal is twofolds. (i) The gap is dynamical, e.g., it can be switched on and off as the laser is turned on and off, which may lead to possible quantum coherent manipulation. (ii) The gap opening term appears at the lowest order. This is in contrast to the case of static magnetic fields, where a gap appears at the third order and other perturbation terms may lead to unwanted effects. We will show that the integrability of the system with the laser-induced lowest-order term is maintained. From the theoretical viewpoint, this nature is important to analytically understand the laser-driven physics.

The laser-driven gapped state is a spin-liquid version of the “Floquet topological insulator” [14–17]. In the state, a chiral edge mode of Majorana fermions [8] appears as indicated in Fig. 1(a). The direction of this mode can

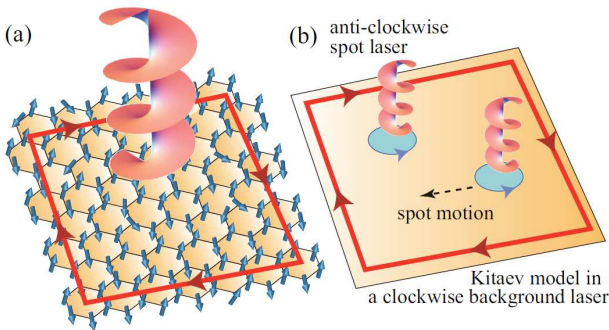


FIG. 1: (color online) Kitaev model in a circularly or elliptically polarized laser. A chiral Majorana edge mode appears. (b) Manipulation of edge modes by spatially modulated spot laser.

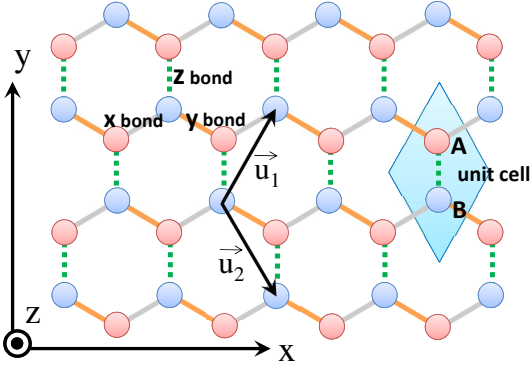


FIG. 2: (color online) Honeycomb lattice of the Kitaev model. There are three types of bonds (x , y , and z bonds). The unit vectors are defined by $\mathbf{u}_1 = \hat{x}/2 + \sqrt{3}\hat{y}/2$ and $\mathbf{u}_2 = \hat{x}/2 - \sqrt{3}\hat{y}/2$, where $\hat{x} = (1, 0)$ and $\hat{y} = (0, 1)$ ($|\mathbf{u}_{1,2}| = 1$). The unit cell consists of two neighboring sites and the system is divided into A and B sublattices.

be switched by altering the helicity of the laser. It is also possible to make islands of topological spin-liquid states using a spatial modulation technique [6, 20] [see Fig. 1(b)]: A spot of EPL leads to a locally topological state in the "sea" of the Kitaev model. The topological island can be spatially manipulated by slowly moving the spot position.

Model – We focus on the Kitaev model with a ME coupling in EPL (see Fig. 1). We assume that the ME coupling originates from electric or phonon-assisted polarization on each bond and its strength is proportional to the exchange interaction of the bond. Then, a quantum spin system responds to an external *electric* field through the polarization tensor. This effect is known as magnetostriction and has been confirmed in various multiferroic materials [32–36]. Our total Hamiltonian is given by

$$\hat{H}(t) = \hat{H}_{\text{Kitaev}} + \hat{H}_{\text{ME}}(t). \quad (1)$$

The first term is the Kitaev Hamiltonian

$$\hat{H}_{\text{Kitaev}} = \sum_{\alpha=x,y,z} J_{\alpha} \sum_{\langle \mathbf{r}, \mathbf{r}' \rangle_{\alpha}} \sigma_{\mathbf{r}}^{\alpha} \sigma_{\mathbf{r}'}^{\alpha}. \quad (2)$$

This model is defined on a honeycomb lattice as displayed in Fig. 2. Here $S_{\mathbf{r}}^{\alpha} = \frac{1}{2}\sigma_{\mathbf{r}}^{\alpha}$ denotes the α component of spin- $\frac{1}{2}$ operator on site \mathbf{r} ($\sigma_{\mathbf{r}}^{x,y,z}$ are Pauli matrices and we set $\hbar = 1$), $\sum_{\langle \mathbf{r}, \mathbf{r}' \rangle_{\alpha}}$ stands for the summation over all neighboring spin pairs on α bonds (see Fig. 2), and J_{α} is the Ising coupling constant of the α bond. In order to describe the ME coupling, we introduce the electric polarization $\mathbf{P}_{(\mathbf{r}, \mathbf{r}')_{\alpha}}$ on each α bond $(\mathbf{r}, \mathbf{r}')_{\alpha}$ proportional to the Ising interaction

$$\mathbf{P}_{(\mathbf{r}, \mathbf{r}')_{\alpha}} = \boldsymbol{\pi}_{\alpha} \sigma_{\mathbf{r}}^{\alpha} \sigma_{\mathbf{r}'}^{\alpha}, \quad (3)$$

where $\boldsymbol{\pi}_{\alpha}$ is the ME-coupling vector. Using the total polarization $\mathbf{P}_{\text{tot}} = \sum_{\alpha} \mathbf{P}_{\text{tot}, \alpha} = \sum_{\alpha} \sum_{\langle \mathbf{r}, \mathbf{r}' \rangle_{\alpha}} \mathbf{P}_{(\mathbf{r}, \mathbf{r}')_{\alpha}}$,

the ME term becomes

$$\hat{H}_{\text{ME}}(t) = -\mathbf{E}(t) \cdot \mathbf{P}_{\text{tot}}. \quad (4)$$

We assume that the electric field vector \mathbf{E} of the EPL is in the x - y plane (= plane of the honeycomb lattice) and given by

$$\mathbf{E}(t) = E(\mp \cos(\Omega t + \delta), \sin(\Omega t), 0), \quad (5)$$

where t is time, Ω is the laser frequency, E is the magnitude of field and the signs \mp denote clockwise/anticlockwise rotating laser. The phase δ ($|\delta| \leq \pi/2$) controls the ellipticity; $\delta = 0$ and $\pi/2$ correspond to circularly and linearly polarized laser, respectively. We note that laser has a magnetic field component that couples to spin systems via Zeeman interaction. However, we can ignore this because the magnetic fields are much weaker than the electric fields in electromagnetic waves.

Floquet theory and $1/\Omega$ expansion – The Hamiltonian of Eq. (1) is temporally periodic: $\hat{H}(t + T) = \hat{H}(t)$ with $T = 2\pi/\Omega$. The Floquet theorem, i.e., temporal version of the Bloch theorem, states that the time-dependent Schrödinger equation $i\partial_t |\Psi(t)\rangle = \hat{H}(t) |\Psi(t)\rangle$ can be mapped to an effective *static* eigenvalue problem $\sum_n (\hat{H}_{m-n} - m\Omega \delta_{m,n}) |\Phi^n\rangle = \epsilon |\Phi^m\rangle$, which can be proved by Fourier transform $|\Phi^m\rangle = T^{-1} \int dt e^{im\Omega t} |\Phi(t)\rangle$ and $\hat{H}_m = T^{-1} \int dt e^{im\Omega t} \hat{H}(t)$. The time periodic Floquet state $|\Phi(t)\rangle (= |\Phi(t + T)\rangle)$ is related to the solution of the time-dependent Schrödinger equation via $|\Psi(t)\rangle = e^{-i\epsilon t} |\Phi(t)\rangle$ (ϵ is called the Floquet quasi-energy). In the present case, we have $\hat{H}_0 = \hat{H}_{\text{Kitaev}}$, $\hat{H}_{+1} = -\frac{E}{2}(\mp e^{-i\delta}, i, 0) \cdot \mathbf{P}_{\text{tot}}$, and $\hat{H}_{-1} = -\frac{E}{2}(\mp e^{i\delta}, -i, 0) \cdot \mathbf{P}_{\text{tot}}$. Terms $\hat{H}_{\pm p}$ with $p \geq 2$ are zero.

We consider the case where Ω is much larger than the energy scale of \hat{H}_{Kitaev} (i.e., $|J_{x,y,z}|$). Since the typical energy of spin couplings is in the THz regime (1THz \sim 4meV), this implies that THz or mid-infrared lasers are suitable. Then, each m -photon subspace are energetically isolated from other subspaces and the off-diagonal terms $\hat{H}_{\pm 1}$ can be treated perturbatively. The effective Hamiltonian acting on the 0-photon subspace is given by [15]

$$\hat{H}_{\text{eff}} = \hat{H}_{\text{Kitaev}} - \frac{1}{\Omega} [\hat{H}_{+1}, \hat{H}_{-1}] \quad (6)$$

up to $\mathcal{O}(\Omega^{-1})$. Utilizing Eq. (3), we can show that the first order term $\hat{H}_{\Omega} = -[\hat{H}_{+1}, \hat{H}_{-1}]/\Omega$ results in the following three-spin interactions:

$$\begin{aligned} \hat{H}_{\Omega} = & \pm \frac{1}{\Omega} E^2 \cos \delta \left[G_{12} \left(\sum_{\mathbf{r} \in A} \sigma_{\mathbf{r}_1}^x \sigma_{\mathbf{r}}^z \sigma_{\mathbf{r}_2}^y + \sum_{\mathbf{r} \in B} \sigma_{\mathbf{r}_1}^x \sigma_{\mathbf{r}}^z \sigma_{\mathbf{r}_2}^y \right) \right. \\ & + G_{23} \left(\sum_{\mathbf{r} \in A} \sigma_{\mathbf{r}_2}^y \sigma_{\mathbf{r}}^x \sigma_{\mathbf{r}_3}^z + \sum_{\mathbf{r} \in B} \sigma_{\mathbf{r}_2}^y \sigma_{\mathbf{r}}^x \sigma_{\mathbf{r}_3}^z \right) \\ & \left. + G_{31} \left(\sum_{\mathbf{r} \in A} \sigma_{\mathbf{r}_3}^z \sigma_{\mathbf{r}}^y \sigma_{\mathbf{r}_1}^x + \sum_{\mathbf{r} \in B} \sigma_{\mathbf{r}_3}^z \sigma_{\mathbf{r}}^y \sigma_{\mathbf{r}_1}^x \right) \right]. \quad (7) \end{aligned}$$

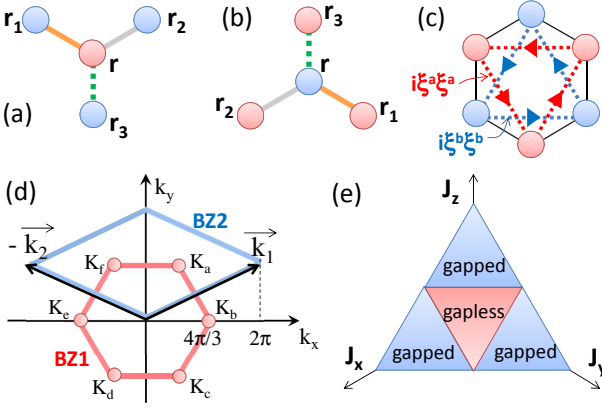


FIG. 3: (color online) Three sites around site $\mathbf{r} \in A$ (a) and around $\mathbf{r} \in B$ (b). (c) NNN coupling in Eq. (11). (d) Brillouin zones (BZ) of the Kitaev model, hexagonal (BZ1) and rhombus (BZ2), where $\mathbf{k}_{1,2}$ are reciprocal lattice vectors. (e) Ground-state phase diagram of $\hat{\mathcal{H}}_{\text{Kitaev}}$ in the plane $J_x + J_y + J_z = 1$ [7, 29].

Here, $G_{\alpha\beta} = \hat{z} \cdot (\boldsymbol{\pi}_\alpha \times \boldsymbol{\pi}_\beta)$ [$\hat{z} = (0, 0, 1)$ and symbol \times denotes outer product], $\sum_{\mathbf{r} \in A(B)}$ summation over sublattice A (B), and the signs \mp corresponds to clockwise/anticlockwise rotating laser respectively. Vectors $\mathbf{r}_{1,2,3}$ are sites around \mathbf{r} as depicted in Fig. 3. Note that $\hat{\mathcal{H}}_\Omega$ is non-zero unless the laser is linearly polarized ($\delta = \pi/2$) or all $\boldsymbol{\pi}_{x,y,z}$ are parallel with each other. This laser-induced three-spin interaction (7) is the main result of this paper and we will discuss its physical outcomes in the following.

Fermionization and Floquet topological state – Here, we study the low-energy effective model (6) by fermionization [7, 29]. Jordan-Wigner transformation maps spin- $\frac{1}{2}$ operators to fermions:

$$2c_r^\dagger c_r - 1 = \sigma_r^z, \quad c_r^\dagger = \frac{1}{2} \left[\prod_{\mathbf{r}' < \mathbf{r}} \sigma_{\mathbf{r}'}^z \right] \sigma_{\mathbf{r}}^+ \quad (8)$$

Here $\sigma_{\mathbf{r}}^\pm = \sigma_{\mathbf{r}}^x \pm i\sigma_{\mathbf{r}}^y$ and $\prod_{\mathbf{r}' < \mathbf{r}} \sigma_{\mathbf{r}'}^z$ is a non-local product whose path is defined in Fig. 2 of Ref. 29. Operators $c_{\mathbf{r}}$ and $c_{\mathbf{r}}^\dagger$ are complex fermions satisfying $\{c_{\mathbf{r}}, c_{\mathbf{r}'}^\dagger\} = \delta_{\mathbf{r}, \mathbf{r}'}$ and $\{c_{\mathbf{r}}, c_{\mathbf{r}'}\} = \{c_{\mathbf{r}}^\dagger, c_{\mathbf{r}'}^\dagger\} = 0$. We define four Majorana (real) fermions

$$\begin{aligned} \xi_{\mathbf{r}}^a &= -i(a_{\mathbf{r}} - a_{\mathbf{r}}^\dagger), & \chi_{\mathbf{r}}^a &= a_{\mathbf{r}} + a_{\mathbf{r}}^\dagger, \\ \chi_{\mathbf{r}}^b &= -i(b_{\mathbf{r}} + b_{\mathbf{r}}^\dagger), & \xi_{\mathbf{r}}^b &= b_{\mathbf{r}} + b_{\mathbf{r}}^\dagger, \end{aligned} \quad (9)$$

where $a_{\mathbf{r}}$ ($b_{\mathbf{r}}$) is a fermion $c_{\mathbf{r}}$ on sublattice A (B). We choose $\xi_{\mathbf{r}}^a$ and $\xi_{\mathbf{r}}^b$ ($\chi_{\mathbf{r}}^a$ and $\chi_{\mathbf{r}}^b$) to be in the same unit cell. Majorana fermions satisfy $\{\xi_{\mathbf{r}}^\alpha, \xi_{\mathbf{r}'}^\beta\} = \{\chi_{\mathbf{r}}^\alpha, \chi_{\mathbf{r}'}^\beta\} = 2\delta_{\alpha,\beta}\delta_{\mathbf{r},\mathbf{r}'}$, $\{\xi_{\mathbf{r}}^\alpha, \chi_{\mathbf{r}'}^\beta\} = 0$, $\xi^\dagger = \xi$ and $\chi^\dagger = \chi$. Using these fermions, the Kitaev Hamiltonian $\hat{\mathcal{H}}_{\text{Kitaev}}$ becomes [37]

$$\hat{\mathcal{H}}_{\text{Kitaev}} = \sum_{\mathbf{r}} iJ_x \xi_{\mathbf{r}}^a \xi_{\mathbf{r}+\mathbf{u}_1}^b - iJ_y \xi_{\mathbf{r}}^b \xi_{\mathbf{r}+\mathbf{u}_2}^a - \hat{I}_{\mathbf{r}} iJ_z \xi_{\mathbf{r}}^b \xi_{\mathbf{r}}^a \quad (10)$$

where $\mathbf{r} = n_1 \mathbf{u}_1 + n_2 \mathbf{u}_2$ ($n_{1,2}$: integer), $\sum_{\mathbf{r}}$ runs over the unit cells. The χ fermion appears in the Hamiltonian through a locally conserved operator $\hat{I}_{\mathbf{r}} = i\chi_{\mathbf{r}}^a \chi_{\mathbf{r}}^b$ with an eigenvalue ± 1 . In the ground state of $\hat{\mathcal{H}}_{\text{Kitaev}}$, it is known [7, 29, 38] that we can set all $\hat{I}_{\mathbf{r}}$ to be unity (or -1) and vortex-type excitations defined by sign flips of $\hat{I}_{\mathbf{r}}$ are gapped (i.e., fermions $\chi^{a,b}$ are gapped). We will set $\hat{I}_{\mathbf{r}} = 1$ hereafter.

The laser-induced three-spin interaction (7) can be fermionized as well and results in

$$\begin{aligned} \hat{\mathcal{H}}_\Omega &= \pm \frac{1}{\Omega} E^2 \sum_{\mathbf{r}} iG_{12} \left[\xi_{\mathbf{r}}^b \xi_{\mathbf{r}+\mathbf{u}_1+\mathbf{u}_2}^b + \xi_{\mathbf{r}}^a \xi_{\mathbf{r}-\mathbf{u}_1-\mathbf{u}_2}^a \right] \\ &+ i\hat{I}_{\mathbf{r}} G_{23} \left[\xi_{\mathbf{r}}^b \xi_{\mathbf{r}-\mathbf{u}_2}^b + \xi_{\mathbf{r}}^a \xi_{\mathbf{r}+\mathbf{u}_2}^a \right] \\ &+ i\hat{I}_{\mathbf{r}} G_{31} \left[\xi_{\mathbf{r}}^b \xi_{\mathbf{r}-\mathbf{u}_1}^b + \xi_{\mathbf{r}}^a \xi_{\mathbf{r}+\mathbf{u}_1}^a \right]. \end{aligned} \quad (11)$$

The Kitaev Hamiltonian (10) represents nearest neighbor hopping, while $\hat{\mathcal{H}}_\Omega$ describes an imaginary NNN hopping as displayed in Fig. 3(c) [39].

To see the spectral nature in the $\hat{I}_{\mathbf{r}} = 1$ sector, we move to the momentum \mathbf{k} space using Fourier transforms $\xi_{\mathbf{r}}^{a(b)} = \sqrt{2/N} \sum_{\mathbf{k}} [e^{i\mathbf{k}\cdot\mathbf{r}} \xi_{\mathbf{k}}^{a(b)} + e^{-i\mathbf{k}\cdot\mathbf{r}} \xi_{\mathbf{k}}^{a(b)\dagger}]$. Here $\sum'_{\mathbf{k}}$ stands for summation over *half* the Brillouin zone (BZ) and N is the total number of unit cells. We can choose either hexagonal or rhombus form as the BZ shown in Fig. 3(d). Fermions in the \mathbf{k} space are of complex type, and satisfy $\{\xi_{\mathbf{k}}^\alpha, \xi_{\mathbf{k}'}^\beta\} = \delta_{\alpha,\beta} \delta_{\mathbf{k},\mathbf{k}'}$ and $\{\xi_{\mathbf{k}}^\alpha, \xi_{\mathbf{k}'}^\beta\} = 0$. We can denote $\hat{\mathcal{H}}_{\text{eff}} = \sum'_{\mathbf{k}} \Xi_{\mathbf{k}}^\dagger \mathcal{H}_{\mathbf{k}} \Xi_{\mathbf{k}}$, where $\Xi_{\mathbf{k}} = {}^t(\xi_{\mathbf{k}}^a, \xi_{\mathbf{k}}^b)$ and the 2×2 matrix $\mathcal{H}_{\mathbf{k}}$ is given by

$$\mathcal{H}_{\mathbf{k}} = \sum_{\alpha=x,y,z} h_{\mathbf{k}}^\alpha \tau^\alpha. \quad (12)$$

Here $\tau^{x,y,z}$ are Pauli matrices, $h_{\mathbf{k}}^x = -2(J_x \sin(\mathbf{k} \cdot \mathbf{u}_1) - J_y \sin(\mathbf{k} \cdot \mathbf{u}_2))$, $h_{\mathbf{k}}^y = -2(J_x \cos(\mathbf{k} \cdot \mathbf{u}_1) + J_y \cos(\mathbf{k} \cdot \mathbf{u}_2) + J_z)$ and $h_{\mathbf{k}}^z = \pm \frac{4}{\Omega} E^2 \cos \delta [G_{12} \sin(\mathbf{k} \cdot (\mathbf{u}_1 + \mathbf{u}_2)) - G_{23} \sin(\mathbf{k} \cdot \mathbf{u}_2) - G_{31} \sin(\mathbf{k} \cdot \mathbf{u}_1)]$. We stress that EPL gives a non-zero z -component $h_{\mathbf{k}}^z$. The Hamiltonian (12) can be diagonalized leading to dispersions

$$E_{\mathbf{k}}^\pm = \pm (|h_{\mathbf{k}}^x|^2 + |h_{\mathbf{k}}^y|^2 + |h_{\mathbf{k}}^z|^2)^{1/2}. \quad (13)$$

We plot the energy spectrum for the zero field case ($E = 0$) at $J_x = J_y = J_z$ in Fig. 4(a). We see gapless Dirac cones appearing at the six corners $K_{a,\dots,f}$ of BZ1. However, since we defined two complex fermions in momentum space from two real ones $\xi_{\mathbf{r}}^{a,b}$, there is a redundancy and we should restrict ourselves to half the BZ [e.g., the right triangular area of BZ2 in Fig. 3(d)]. Thus, only gapless excitations around a single Dirac point (e.g., K_a) describes the low-energy physics of the Kitaev model. The gapless Dirac cone exists if the condition $|J_\alpha| \leq |J_\beta| + |J_\gamma|$ [7] is satisfied (α, β and γ are all different). The ground-state phase diagram of the Kitaev model is summarized as in Fig. 3(e). In the gapped

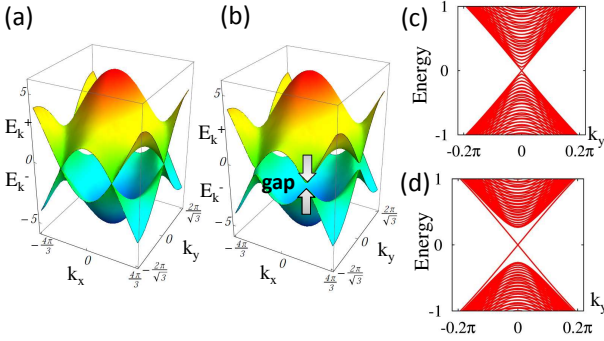


FIG. 4: (color online) (a)(b) Fermion dispersions of the effective model (6) in the $\hat{I}_r = 1$ sector under, and (c)(d) is the spectrum in cylindrical geometry with an armchair edge along the y direction. Panels (a) and (c) [(b) and (d)] are results for the zero electric field case ($E = 0$) [a finite-field case ($4E^2\Omega^{-1}\cos\delta = 0.1$)]. Two gapless modes connecting the bulk continuum in panel (d) correspond to chiral edge modes along the y direction. $J_{x,y,z} = 1$ and $G_{12,23,31} = 1$ are used.

phase, vortex excitations of $\chi^{a,b}$ are regarded as Abelian anyons [7].

Next, we move to the finite field case $E \neq 0$. We show that $\hat{\mathcal{H}}_\Omega$ plays the role similar to the NNN hopping in the Haldane honeycomb model [11]. The energy dispersion is plotted in Fig. 4(b). The laser-induced NNN hopping opens a finite gap at the Dirac point in the gapless phase. Let us investigate the topological nature of the laser-driven gapped state. To this end, we first focus on the low-energy physics around the Dirac point K_a . The Hamiltonian matrix near $\mathbf{k}_a = (2\pi/3, 2\pi/\sqrt{3})$ is given by ($J_{x,y,z} = J$)

$$\mathcal{H}_{\mathbf{k}_a + \delta\mathbf{k}} = \begin{pmatrix} m & \sqrt{3}J(i\delta k_x + \delta k_y) \\ \sqrt{3}J(-i\delta k_x + \delta k_y) & -m \end{pmatrix} \quad (14)$$

up to linear order in $\delta\mathbf{k} = \mathbf{k} - \mathbf{k}_a$. The mass parameter is $m = \pm 2\sqrt{3}E^2\Omega^{-1}\cos\delta(G_{12} + G_{23} + G_{31})$ and its sign \pm corresponds to clockwise/anticlockwise rotation of laser. This is nothing but a Hamiltonian for a $(2+1)$ -dimensional Dirac fermion with a gap $2m$. The mass m is generally non-zero except for $\delta = \pi/2$ or $G_{12} + G_{23} + G_{31} = 0$. It is known that a massive Dirac fermion exhibits an anomalous quantized "Hall" effect without Landau levels [11]. Therefore, Eq. (14) indicates that a gapless chiral edge mode of Majorana fermions is induced by EPL and its direction can be changed by inverting the helicity of the laser. We stress that the present edge mode is chargeless in contrast to the case of integer quantum Hall effects (IQHE). In Figs. 4 (c) and (d), we explicitly show the energy levels of the Kitaev model in EPL defined on a cylinder geometry with an armchair edge along the y direction. When the field is turned on, we see the gap opening as well as a formation of the edge mode. We confirmed that

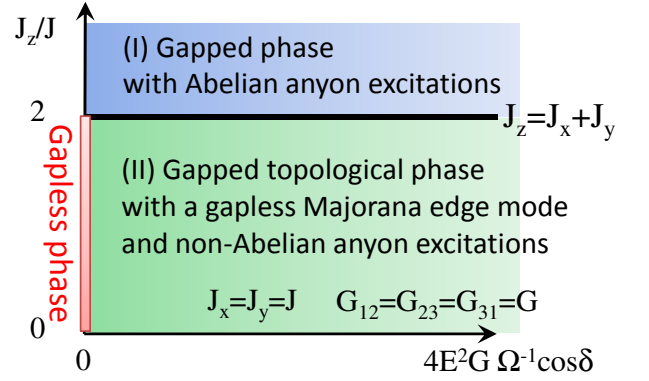


FIG. 5: (color online) Nonequilibrium phase diagram of the effective Hamiltonian (6) in the space of $J_{x,y} = J$ and $G_{12,23,31} = G$. This diagram becomes accurate at $\Omega \gg |J_{x,y,z}|$.

the edge mode is stable against small change of $J_{x,y,z}$ and E . This edge mode is a Majorana type. This can be confirmed by mapping $\hat{\mathcal{H}}_{\text{eff}}$ to a Bogoliubov-de Gennes (BdG) Hamiltonian for topological superconductor through new fermions $d_r = (\xi_r^a + i\xi_r^b)/2$ [29]. The dispersion of the BdG Hamiltonian on a cylinder geometry has a gapless edge mode, which clearly shows the presence of a Majorana edge mode [8]. It is known [7] that the laser-induced topological phase has gapped non-Abelian anyon excitations originating from fermions $\chi^{a,b}$.

The phase diagram of the effective Hamiltonian (6) is summarized in Fig. 5. Phase II corresponds to the laser-driven gapped phase with a gapless Majorana edge mode. It is possible to generate islands of the topological spin liquid state by applying spot laser as shown in Fig. 1(b). Their position can be changed by slowly moving the spot positions. On the line $J_z = 2J$, a nonequilibrium phase transition occurs in which two Dirac points $K_{a,f}$ merge at $\mathbf{k}' = (0, 2\pi/\sqrt{3})$.

Finally, we shortly discuss the detection scheme for the gapless chiral edge mode. As in other topological states, the edge state can be observed through transport measurements. Thermal transport is appropriate since the present edge mode is chargeless. At sufficiently low temperatures T , the thermal conductance along an edge is [7, 40, 41]

$$G_{\text{th}} = \frac{\pi k_B^2}{12} T. \quad (15)$$

We emphasize that G_{th} is half compared to IQHE because the edge mode is formed by Majorana fermions.

Conclusions – We have studied laser-induced nonequilibrium states of the Kitaev model making use of the Floquet theory. When EPL is applied, we showed that a topological spin-liquid state with a gapless Majorana edge mode is generated if the effect of magnetostriction ME coupling is considered. The laser-induced gap and

the direction of the edge current can be controlled by changing the strength and helicity of laser.

MS deeply thanks Ken Shiozaki for discussions about topological superconductors. MS is also thankful to Ken Funo, Nobuo Furukawa, Masahito Mochizuki, and Sei Suzuki for several discussions. MS is supported by KAKENHI (Grants No. 25287088, 26870559), and TO by KAKENHI (Grant No. 23740260, 24224009).

-
- [1] A. V. Kimel, A. Kirilyuk, P. A. Usachev, R. V. Pisarev, A. M. Balbashov, and T. Rasing, *Nature* **435**, 655 (2005).
- [2] A. Kirilyuk, A. V. Kimel, and T. Rasing, *Rev. Mod. Phys.* **82**, 2731 (2010).
- [3] J. Karch, P. Olbrich, M. Schmalzbauer, C. Zoth, C. Brinsteiner, M. Fehrenbacher, U. Wurstbauer, M. M. Glazov, S. A. Tarasenko, E. L. Ivchenko, D. Weiss, J. Eroms, R. Yakimova, S. Lara-Avila, S. Kubatkin, S. D. Ganichev, *Phys. Rev. Lett.* **105**, 227402 (2010).
- [4] J. Karch, C. Drexler, P. Olbrich, M. Fehrenbacher, M. Hirmer, M. M. Glazov, S. A. Tarasenko, E. L. Ivchenko, B. Birkner, J. Eroms, D. Weiss, R. Yakimova, S. Lara-Avila, S. Kubatkin, M. Ostler, T. Seyller, and S. D. Ganichev, *Phys. Rev. Lett.* **107**, 276601 (2011).
- [5] Y. H. Wang, H. Steinberg, P. Jarillo-Herrero, and N. Gedik, *Science* **342**, 453 (2013).
- [6] N. Gedik, J. Orenstein, R. Liang, D. A. Bonn, and W. N. Hardy, *Science* **300**, 1410 (2003).
- [7] Y. A. Kitaev, *Ann. Phys.* **321**, 2 (2006).
- [8] N. Read and D. Green, *Phys. Rev. B* **61**, 10267 (2000).
- [9] D. A. Ivanov, *Phys. Rev. Lett.* **86**, 268 (2001).
- [10] C. Nayak, S. H. Simon, A. Stern, M. Freedman, S. Das Sarma, *Rev. Mod. Phys.* **80**, 1083 (2008).
- [11] F. D. M. Haldane, *Phys. Rev. Lett.* **61**, 2015 (1988).
- [12] C. L. Kane, and E. J. Mele, *Phys. Rev. Lett.* **95**, 146802 (2005).
- [13] B. A. Bernevig, T. L. Hughes, and S.-C. Zhang, *Science* **314**, 1757 (2006).
- [14] T. Oka and H. Aoki, *Phys. Rev. B* **79**, 081406(R) (2009).
- [15] T. Kitagawa, T. Oka, A. Brataas, L. Fu, and E. Demler, *Phys. Rev. B* **84**, 235108 (2011).
- [16] Z. Gu, H. A. Fertig, D. P. Arovas, and A. Auerbach, *Phys. Rev. Lett.* **107**, 216601 (2011).
- [17] N. H. Lindner, G. Refael, and V. Galitski, *Nat. Phys.* **7**, 490 (2011).
- [18] B. Dóra, J. Cayssol, F. Simon, and R. Moessner, *Phys. Rev. Lett.* **108**, 056602 (2012).
- [19] M. S. Rudner, N. H. Lindner, E. Berg, and M. Levin, *Phys. Rev. X* **3**, 031005 (2013).
- [20] Y. T. Katan and D. Podolsky, *Phys. Rev. Lett.*, **110**, 016802, (2013).
- [21] M. C. Rechtsman, J. M. Zeuner, Y. Plotnik, Y. Lumer, D. Podolsky, F. Dreisow, S. Nolte, M. Segev, and A. Szameit, *Nature* **496**, 196 (2013).
- [22] S. Takayoshi, M. Sato, and T. Oka, arXiv:1402.0881.
- [23] S. Takayoshi, H. Aoki, and T. Oka, arXiv:1302.4460.
- [24] L. Jiang, T. Kitagawa, J. Alicea, A. R. Akhmerov, D. Pekker, G. Refael, J. I. Cirac, E. Demler, M. D. Lukin, and P. Zoller, *Phys. Rev. Lett.* **106**, 220402 (2011).
- [25] G. Liu, N. Hao, S.-L. Zhu, and W. M. Liu, *Phys. Rev. A* **86**, 013639 (2012).
- [26] D. E. Liu, A. Levchenko, and H. U. Baranger, *Phys. Rev. Lett.* **111**, 047002 (2013).
- [27] A. Kundu, B. Seradjeh, *Phys. Rev. Lett.* **111**, 136402 (2013).
- [28] Although chiral edge states were observed, it is highly likely that experiments [3, 4] are in the classical limit of Hall effect.
- [29] H.-D. Chen and Z. Nussinov, *J. Phys. A: Math. Theor.* **41**, 075001 (2008).
- [30] G. Jackeli and G. Khaliullin, *Phys. Rev. Lett.* **102**, 017205 (2009).
- [31] J. Chaloupka, G. Jackeli, and G. Khaliullin, *Phys. Rev. Lett.* **105**, 027204 (2010).
- [32] See, for a review of multiferroics, K. F. Wang, J.-M. Liu, and Z. F. Ren, *Advances in Physics* **58**, 321 (2009).
- [33] A. Pimenov, A. A. Mukhin, V. Yu. Ivanov, V. D. Travkin, A. M. Balbashov, and A. Loidl: *Nature Physics* **2**, 97 (2006).
- [34] S. Miyahara and N. Furukawa, arXiv:0811.4082.
- [35] M. Mochizuki, N. Furukawa, and N. Nagaosa, *Phys. Rev. Lett.* **104**, 177206 (2010).
- [36] S. Furukawa, M. Sato, and S. Onoda, *Phys. Rev. Lett.* **105**, 257205 (2010).
- [37] In the original work, Kitaev used a different method than the Jordan-Wigner transformation (see Ref. 7 for details).
- [38] It is numerically shown in Ref. 7 that the energy of \hat{H}_{Kitaev} is minimized when all \hat{I}_r are set to be unity or -1 (see Appendix A of Ref. 7). On the other hand, if the fermionized Hamiltonian (10) has a "reflection" symmetry (e.g., the case of $J_x = J_y$), we can rigorously prove the above statement on minimizing the energy by applying Lieb's theorem: E. H. Lieb, *Phys. Rev. Lett.* **73**, 2158 (1994).
- [39] When a laser is applied to the Kitaev model, $-\mathbf{E} \cdot \mathbf{P}_{\text{tot}}$ acts on its quantum states. If we initially set $\hat{I}_r = 1$, the above operator does not induce any sign flip of \hat{I}_r because exchange couplings $\sigma_r^x \sigma_{r'}^x$, $\sigma_r^y \sigma_{r'}^y$, and $\sigma_r^z \sigma_{r'}^z$ in \mathbf{P}_{tot} are respectively proportional to $i\xi_r^a \xi_{r+u_1}^b$, $-i\xi_r^a \xi_{r+u_2}^b$ and $-i\hat{I}_r \xi_r^a \xi_r^b$ [see Eq. (10)].
- [40] C. L. Kane and M. P. A. Fisher, *Phys. Rev. B* **55**, 15832 (1997).
- [41] A. Cappelli, M. Huerta and G. R. Zemba, *Nucl. Phys. B* **636**, 568 (2002).